ANL/RA/CP-95551

Principal Author: Temitope A. Taiwo
Argonne National Laboratory
9700 South Cass Avenue,
Argonne, Il 60439

Phone: (630) 252 1387
Fax: (630) 252 4500
E-mail Taiwo@anl.gov

Title:
Analysis of ANS LWR Physics Benchmark Problems

Contributing Authors:
T. A. Taiwo, R. N. Blomquist, G. Palmiotti, and J. R. Deen

for presentation at
The International Conference on the Physics of
Nuclear Science and Technology
Long Island, NY, October 1998

Intended Session:
Reactor Physics Benchmarks (POSTER SESSION)

INVITED PAPER
Paper Number: 46

Work Supported by the U. S. Department of Energy, Nuclear Energy Program under Contract W-31-109-ENG-38.

DISCLAIMER

DISCLAIMER

Portions of this document may be illegible in electronic image products. Images are produced from the best available original document.

ANALYSIS OF ANS LWR PHYSICS BENCHMARK PROBLEMS

Temitope A. Taiwo
Argonne National Laboratory
Argonne, IL 60439, U.S.A

Roger N. Blomquist
Argonne National Laboratory
Argonne, IL 60439, U.S.A

Giuseppe Palmiotti
Argonne National Laboratory
Argonne, IL 60439, U.S.A

James R. Deen
Argonne National Laboratory
Argonne, IL 60439, U.S.A.

ABSTRACT

Various Monte Carlo and deterministic solutions to the three PWR Lattice Benchmark Problems recently defined by the ANS Ad Hoc Committee on Reactor Physics Benchmarks are presented. These solutions were obtained using the VIM continuous-energy Monte Carlo code and the DIF3D/WIMS-D4M code package implemented at the Argonne National Laboratory. The code results for the k_{eff} and relative pin power distribution are compared to measured values. Additionally, code results for the three benchmark-prescribed infinite lattice configurations are also intercompared. The results demonstrate that the codes produce very good estimates of both the k_{eff} and power distribution for the critical core and the lattice parameters of the infinite lattice configuration.

I. INTRODUCTION

The PWR Lattice Benchmark Problems[1] were defined by the ANS Ad Hoc Committee on Reactor Physics Benchmarks in mid-1996, as a means of intercomparing and validating various calculation methodologies and codes used for analyzing light water reactor (LWR) cores. The benchmark problems were derived from "clean" LWR critical experiments performed at the Babcock and Wilcox (B&W) Lynchburg Research Center in the early 1970s,[2] and involve three of the nineteen core loadings described in Ref. 2.

In this paper, we discuss the different approaches taken by the Argonne National Laboratory benchmark participants to generate the results contributed to the benchmark exercise. These calculation methodologies included continuous-energy Monte Carlo solutions, and deterministic solutions using lattice physics and transport and diffusion theory codes. We also intercompare results obtained using these approaches with experimental data. We demonstrate through these comparisons the accuracy of the VIM[3] Monte Carlo code using ENDF/B-V library. We also show that the computationally inexpensive deterministic approaches using DIF3D nodal diffusion[4] and transport[5] codes with ENDF/B-V based, WIMS-D4M[6]-generated group constants give benchmark quality solutions for the benchmark problems.

II. DESCRIPTION OF EXPERIMENTS AND BENCHMARK PROBLEMS

The critical experiments were performed in an aluminum tank containing UO_2 fuel pins, varying amounts of non-fueled or absorber pins, and borated water at 20°C. The core region of the three cases specified in the benchmark consists of a central 3X3 assembly region surrounded by a driver region of fuel pins of same design as the fuel pins in the assemblies. In each of the three cases, the nine assemblies are of the same type, and each assembly contains 15X15 pin locations. The assembly type is however case dependent. The degree of heterogeneity within the assembly also varies from case to case, with the first of the three benchmark cases containing 225 fuel pins and designated assembly type A, the second containing 208 fuel pins and 17 vacant locations or water holes (type B), and the third (type C) containing 208 fuel pins, one central water hole and 16 pyrex absorber pins. The assembly loading for assembly types B and C are displayed in Figs. 1 and 2.

The benchmark specifications are defined for two-dimensional analysis, with an axial buckling value of 0.00037 cm^{-2} specified for the three cases to account for axial leakage. Adequate specifications are however provided to permit explicit three dimensional calculations. The power distribution measurements in the central assembly and associated experimental uncertainties are

also provided for cases B and C. The requested benchmark results include the predicted k_{eff} for the critical core configurations and normalized power distributions in the central assembly for cases B and C. Certain infinite lattice (unit assembly) physics parameters are also required for understanding potential differences in calculation results.

III. CALCULATION METHODOLOGIES

Various physics codes available at Argonne were used for analyzing these benchmark problems. We submitted to the benchmark exercise results obtained using the VIM[3] Monte Carlo code, and those obtained using the DIF3D nodal diffusion and transport codes, (DIF3D-NODAL[4] and VARIANT,[5] respectively), with group constants generated by the WIMS-D4M[6] code. Some other codes, such as TWODANT,[7] CASMO-3[8] and MCNP,[9] were also employed for in-house comparison.

Benchmark solutions were generated for the critical core configurations and for the numerical unit assembly lattice problems defined for the exercise. The VIM solutions for the critical core configurations were performed with an explicit 3-D model and the continuous energy option based on the ENDF/B-V library. The VIM solution for the unit assembly problems were generated with a 2-D model, since only infinite lattice parameters are required in these problems.

The DIF3D nodal diffusion and transport calculations for the critical core configurations were performed with a 2-D model employing the specified axial buckling value, in keeping with the original intent of the benchmark exercise. The DIF3D unit assembly calculations were also performed with the 2-D model but using a buckling value of zero. These deterministic DIF3D nodal calculations used 15 neutron energy groups and one node per fuel, water-hole or absorber cell in order to provide benchmark quality solutions. This level of detail is more than that used in industry to model LWR reactors; generally, two neutron groups and one or four nodes per *assembly* are employed in nodal codes.

The WIMS-D4M code with its 69-group ENDF/B-V based library was employed in generating the 15 broad group constants used in the DIF3D transport and diffusion theory calculations. Standard procedures[6] for generating cell group constants were followed. Comparisons of the WIMS-D4M-calculated and VIM-edited macroscopic cross sections for the cells indicated that the cross sections generated by WIMS-D4M closely matches those from VIM, showing the applicability of the WIMS-D4M cross sections for LWR calculations. The application of these group constants in the critical core and unit assembly calculations required an homogenization procedure, particularly for the heterogeneous assembly type C, which contained pyrex absorbers. For this case, the homogenization effect was accurately represented in the core calculations employing homogeneous cell cross sections by determining heterogeneity-corrected group constants for the pyrex absorber cell from an iterative process in which it was required that the pyrex cell absorption rate calculated by a reference heterogeneous calculation be reproduced in the calculations using homogeneous-cell group constants. A DIF3D(VARIANT)-transport model, which explicitly represents the pyrex rod and cell water, was used for generating the reference heterogeneous solution in this procedure of absorption rate matching. In the future, we intend to repeat the benchmark exercise using the lattice code DRAGON[10] in connection with an ENDF/B-VI library. It is anticipated that by using the homogenization option of DRAGON, the cumbersome homogenization scheme described above could be avoided while retaining similar accuracy, or better.

IV. INTERCOMPARISON OF RESULTS

A. Core Calculations

Table 1 summarizes the results for the core calculations. The core k_{eff} for the three benchmark cases as calculated by the ANL codes, along with previously published MNCP[11] and PDQ-7/EPRI-CELL[12] results, are displayed in Table 1(a). For each of the three cases, the experimental k_{eff} is 1.0007 ± 0.0006. It is evident from the results presented that the ANL codes produced very accurate k_{eff} values. The generally better accuracy of the deterministic (transport and diffusion theory) solutions may be due to the cancellation of errors and the fact that the Monte Carlo codes (VIM and MCNP) mock-up the experiments in 3-D, and hence those solutions may include axial heterogeneity effects that are neglected in the 2-D solutions. The adequacy of two-group neutron diffusion theory is shown by the PDQ-7/EPRI-CELL results. It should be noted that similarly accurate solutions were produced by Westinghouse calculations of the critical experiments, using the PHOENIX lattice code and the ANC nodal diffusion theory code.[13] Taken as a whole, these results indicate the accuracy to which state-of-the-art codes can predict the critical k_{eff} of beginning-of-life LWR cores.

Table 1(b) is a summary of percent differences between measured and calculated peak-to-average pin

powers (δ_{peak}) in the central assembly of cases B and C. Not shown is the fact that the ANL codes predicted the same peak power locations as recorded by experiment. Also included for comparison in the Table is the root-mean-square (RMS) deviation of the calculated powers from the measured values for the cases. These results show that the accuracy of the ANL codes is comparable to those of industry standard codes, and that the codes provide accurate values of the peak-to-average pin power and power distribution in the central assembly of the criticals. A survey of the power distribution comparisons indicated local fractional differences between measured and calculated pin powers to be less than 0.050. The largest difference (about 5%) occurred for case B at a location on the central assembly boundary. The reason for this is unclear, but may be due to the measurement which indicates an unexplained power dip of more than 4% ($\pm$ 0.6%) in this location.

B. Two-Dimensional Unit Assembly Calculations

Table 2 displays the summary of the calculated lattice parameters required by the benchmark specifications. All the codes predicted the physical trends associated with the different loading. For example, comparing Cases A and B, we see that thermal reaction rates are enhanced because of the softer spectrum resulting from the vacant (water-hole) locations in lattice type B. In addition, the codes gave very similar values for the other lattice parameters. If the 2-D VIM results for the lattice parameters are taken as reference values, the other lattice calculations gave k_{inf} values that are within 0.5% of the reference value, with the CASMO-3 solution giving the largest deviation (about 0.45%) for cases A and B, and VARIANT solution giving the largest deviation (0.49%) for case C. Differences between the code results are attributed to differences in both calculation methodologies and cross section representations.

The reasons for the differences in k_{inf} can be determined by comparing the other lattice parameters. This can be done systematically by deriving an approximate expression for k_{inf} in terms of the other lattice parameters, using two-group diffusion theory. This expression can be used to evaluate the change in the k_{inf} arising from changes in the individual lattice parameters. The maximum deviations in the calculated CR, δ^{25}, ρ^{25}, and δ^{28} values, relative to the "reference" VIM results are about 2.5%, 1.0%, 3.5%, and 4.5%, respectively. Using the expression for k_{inf}, we find that the 2.5% deviation in CR has the largest effect (0.57%) on the k_{inf}. The largest deviations in δ^{25}, ρ^{25}, and δ^{28}, change the k_{inf} by about 0.02%, 0.15%, and 0.15%, respectively. The effect on k_{inf} of maximum deviation of 2.72% in f_{pyrex} (obtained with the CASMO-3 calculation), is about 0.2%. The effects of the deviations in the lattice parameter values on the k_{inf} are quite small (as evident from the differences in k_{inf} values), and thus indicate that any of the approaches employed would give acceptable values of the lattice parameters for the critical experiment. Comparisons of the VIM and MCNP lattice results indicated that differences in the lattice parameters calculated by the two codes are generally within 1 to 2 standard deviations of each other, and that the differences are quite small.

The intercomparisons of the unit assembly power distributions for cases B and C, indicated very good agreement between the deterministic solutions and the Monte Carlo solutions. The RMS difference between the Monte Carlo (VIM and MCNP) power distributions is about 0.01. The RMS difference between VIM and DIF3D(VARIANT) power distributions is less than 0.01.

V. SUMMARY AND CONCLUSIONS

The results presented in this work show that VIM and the DIF3D transport and diffusion theory codes using WIMS-D4M-generated cross sections predicted accurate values for the critical core k_{eff} of the ANS LWR Physics Benchmark Problems, with the largest deviation being about 0.4%. Generally, the deterministic, 2-D models provided k_{eff} values in closest agreement with the recorded experimental values. This is likely due to the cancellation of errors arising from the approximations used in such calculations.

The codes also provided very good estimates of the power distributions in the central assembly of the critical experiments, with the root mean square difference being less than 0.02. The peak pin to assembly average powers in the center assembly of the critical experiments were also well predicted.

An intercomparison of the lattice parameters calculated by the VIM and DIF3D codes and comparison of the results to other codes indicated that the lattice parameters were also well predicted. The differences in calculated values between codes are generally of minor significance with respect to their effect on the lattice k_{inf}. These results indicate the applicability of deterministic codes using ENDF/B-V cross section library for analyzing the benchmark cases.

REFERENCES

1. "PWR Lattice Benchmark Problem L1 Specifications", David J. Diamond letter July 19, 1996.

2. M. N. Baldwin and M. E. Stern, "Physics Verification Program, Part III, Task 4, Summary Report", BAW-3647-20, Babcock and Wilcox, March 1971.

3. R. N. Blomquist, "VIM - A Continuous energy Neutronics and Photon Transport Code," *Intl. Topl. Mtg. Adv. in Mathematics, Computations and Reactor Physics,* April 28-May 2, 1992, Pittsburgh, PA.

4. R. D. Lawrence, "The DIF3D Nodal Neutronics Option for Two- and Three-Dimensional Diffusion Theory Calculations in Hexagonal Geometry," ANL-83-1, Argonne National Laboratory, March 1993.

5. G. Palmiotti, E. E. Lewis, and C. B. Carrico, "VARIANT: VARIational Anisotropic Nodal Transport for Multidimensional Cartesian and Hexagonal Geometry Calculations," ANL-95/40, Argonne National Laboratory, October 1995.

6. J. R. Deen, W. L. Woodruff, and C. I. Costescu, "WIMS-D4M User Manual, Rev. 1," ANL/RERTR/TM-23, Argonne National Laboratory, April 1997.

7. R.E. Alcouffe, F.W. Brinkley, D.R. Marr, and R.D. O'Dell, "User's Guide for TWODANT: A Code Package for Two-Dimensional, Diffusion-Accelerated, Neutral-particle Transport," LA-10049-M, Los Alamos National Laboratory, Feb. 1990.

8. M. Edenius and B. H. Forssen, "CASMO-3, A Fuel Assembly Burnup Program," STUDSVIK/NFA-89/3, June 1993.

9. J. F. Briesmeister, et al., "MCNP - A General Monte Carlo Code for Neutron and Photon Transport," LA-7396-M, Rev. 2, Sept. 1993.

10. G. Marleau, A. Hebert and R. Roy, "A User's Guide for DRAGON, Version DRAGON_971124, Release 3.02," Ecole Polytechnique de Montreal, December, 1997.

11. Russell D. Mosteller and Denise B. Pelowitz, "Critical Lattices of UO2 Fuel Rods and Perturbing Rods in Borated Water", LA-UR-95-1434, Los Alamos National Laboratory, 1995.

12. R. D. Mosteller et al., "Benchmarking of the ARMP System Against Large-Scale Mockup Experiments," *Trans. Am. Nucl. Soc.* 30, 690, Nov. 1978.

13. T. Q. Nguyen, et al., "Benchmarking of the PHOENIX-P/ANC Advanced Nuclear Design System," *Intl. Reactor Physics Conf.*, Vol. III, pg. III-41, Jackson Hole wyoming-September 18-22, 1988.

Table 1. Summary of Results for the Critical Core Calculations.

Table 1(a). Comparison of k_{eff}.			
Code	Case A	Case B	Case C
VIM (ENDF/B-V)	0.9978 ± 0.0003	0.99788 ± 0.00007	0.99823 ± 0.00006
VARIANT	1.00028	1.00137	0.99977
DIF3D-NODAL	0.99967	1.00154	0.99635
MCNP (ENDF/B-V)[11]	0.9976 ± 0.0007	1.0003 ± 0.0007	0.9974 ± 0.0007
PDQ-7/EPRI-CELL[12]	0.9998	1.0018	0.9998

Table 1(b). Comparison of Peak-to-Average Pin Power Ratios.				
Approach	Case B		Case C	
	δ_{peak}(%)	RMS	δ_{peak}(%)	RMS
Measurement	-	0.013*	-	0.011*
VIM	-0.45	0.018	-0.35	0.014
VARIANT	0.18	0.017	1.82	0.017
DIF3D-NODAL	0.18	0.019	0.86	0.014
ANC/PHOENIX[13]	-	-	-0.69	0.014
PDQ-7/EPRI-CELL[12]	0.81	-	2.85	-

*The standard deviation in the measured average pin power

Table 2. Comparison of Unit Assembly Lattice Parameters.

Table 2(a). Comparison of Lattice Parameters for Case A.

	VIM	MCNP	VARIANT/WIMS-D4M	CASMO-3
k_{inf}	1.0578 ± 0.0025	1.0575 ± 0.0011	1.05637	1.06225
δ^{25}	0.1316 ± 0.0007	0.1324 ± 0.0004	0.1306	0.1313
δ^{28}	0.0639 ± 0.0010	0.0644 ± 0.0002	0.0661	0.0667
ρ^{25}	0.3462 ± 0.0022	0.3466 ± 0.0011	0.3536	0.3447
ρ^{28}	2.2507 ± 0.0162	2.2808 ± 0.0080	2.3211	2.2463
CR	0.4717 ± 0.0025	0.4680 ± 0.0013	0.4727	0.4599

Table 2(b). Comparison of Lattice Parameters for Case B.

	VIM	MCNP	VARIANT/WIMS-D4M	CASMO-3
k_{inf}	1.0495 ± 0.0002	1.0497 ± 0.0010	1.04814	1.05438
δ^{25}	0.1168 ± 0.0001	0.1172 ± 0.0003	0.1158	0.1163
δ^{28}	0.0598 ± 0.0002	0.0598 ± 0.0002	0.0591	0.0610
ρ^{25}	0.3072 ± 0.0002	0.3081 ± 0.0011	0.3139	0.3055
ρ^{28}	2.0205 ± 0.0014	2.0340 ± 0.0080	2.0576	1.9980
CR	0.4372 ± 0.0002	0.4389 ± 0.0013	0.4412	0.4306

Table 2(c). Comparison of Lattice Parameters for Case C.

	VIM	MCNP	VARIANT/ WIMS-D4M	TWODANT/ WIMS-D4M	CASMO-3
k_{inf}	0.9906 ± 0.0022	0.9875 ± 0.0012	0.98576	0.98705	0.99416
δ^{25}	0.1294 ± 0.0007	0.1300 ± 0.0004	0.1290	0.1289	0.1282
δ^{28}	0.0660 ± 0.0011	0.0648 ± 0.0002	0.0657	0.0658	0.0657
ρ^{25}	0.3388 ± 0.0028	0.3429 ± 0.0013	0.3502	0.3497	0.3377
ρ^{28}	2.2324 ± 0.0177	2.2641 ± 0.0090	2.3021	2.2989	2.2093
CR	0.4616 ± 0.0026	0.4660 ± 0.0013	0.4701	0.4697	0.4555
f_{pyrex}	0.1396 ± 0.0015	0.1361 ± 0.0007	0.1388	0.1380	0.1434

δ^{25} : Ratio of epithermal-to-thermal ^{235}U fissions.
δ^{28}: Ratio of ^{238}U fissions to ^{235}U fissions.
ρ^{25}: Ratio of epithermal-to-thermal capture in ^{235}U.
ρ^{28}: Ratio of epithermal-to-thermal ^{238}U captures.
CR : ^{238}U captures/^{235}U absorptions.
f_{pyrex} Fraction of total absorption in the pyrex absorber pins.

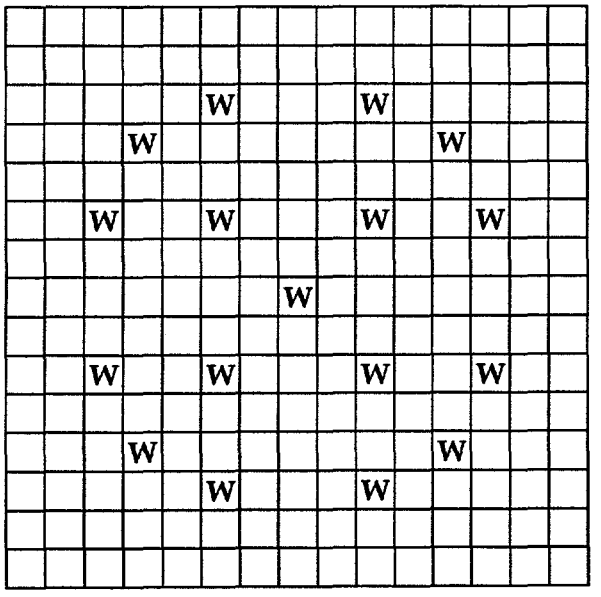

Fig. 1. Assembly Type B

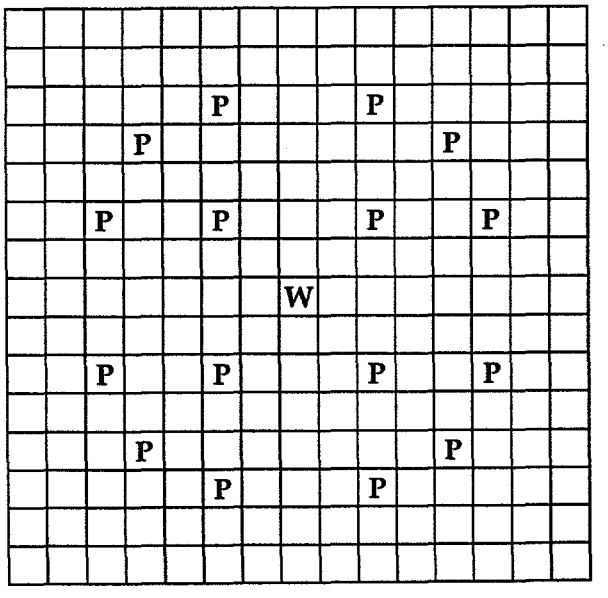

Fig. 2. Assembly Type C